Mode Control in Photonic Crystal Surface Emitting Lasers Through External Reflection

Richard J.E. Taylor, Guangrui Li, Pavlo Ivanov, David T.D. Childs *Member, IEEE*, Timothy S. Roberts, Benjamin J. Stevens, Bret Harrison, Jayanta Sarma, Nasser Babazadeh, Gary Terrnent, and Richard A. Hogg

***Abstract*— In this paper, we show the effect of lateral external optical feedback on an all semiconductor photonic crystal surface emitting laser (PCSEL). Initially a PCSEL is grown and fabricated with a square lattice of triangles, the device is shown to operate electrically driven at room temperature under continuous wave condition. We investigate, theoretically and experimentally, the effect of lateral feedback on the performance of a photonic crystal lasers. Demonstrating a reduction in mode competition, and a modification to spatial mode distribution, opening routes to all electronic beam shaping and divergence control.**

***Index Terms*—Photonic Crystal Lasers, Semiconductor Lasers**

I. Introduction

THERE have been significant recent developments in photonic crystal surface emitting lasers [1,2], with a particular focus on increasing output power through the development of individual lasers [3,4] through photonic crystal design and through coherent laser arrays [5]. Recently, triangular PC features (on a square lattice) have been exploited to realize watt-level output powers [6]. However, such PC structures significantly reduce the frequency difference between modes [7]. Closely spaced modes may lead to mode competition and multimode emission at high powers, both of which are deleterious for most practical laser applications. Utilizing distributed, varying phase feedback introduced through cleaved facets we demonstrate mode control in photonic crystal surface emitting lasers. We are able to show a reduction in threshold, a change in far field, and a switch from multimode to single mode emission.

PCSEL structures generally consist of a photonic crystal layer positioned above the active element within a p-i-n laser structure. Figure 1a shows a schematic representation of a typical PCSEL structure. Through careful design of the photonic crystal (PC) layer it is possible to control the lasing properties, in particular the beam shape [4], and beam polarization [8]. Beam steering has also been demonstrated [9]. PCSELs have previously mainly been realized through wafer fusion [2], however there has been a recent growing trend towards epitaxial overgrowth [10-15].

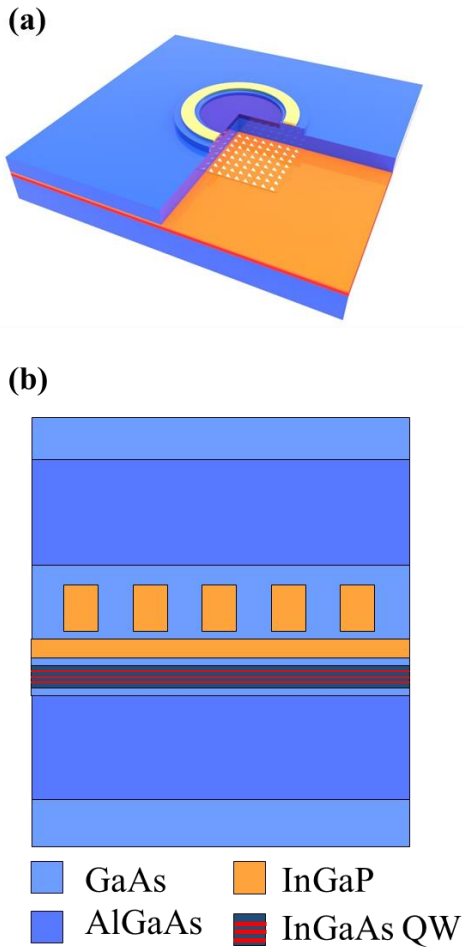

Figure 1 a) three dimensional rendered cut away schematic of PCSEL structure, b) two dimensional schematic of PCSEL layer structure.

"This work was financially supported by the Japan Society for the Promotion of Science (JSPS) under grant P15364 and the Engineering and Physical Sciences Research Council (EPSRC) under grant EP/K023195/1".

R.J.E. Taylor is with the Department of Electrical Engineering and Information Systems, The University of Tokyo, 7-3-1 Hongo, Bunkyo-ku, Tokyo, 113-8656, Japan (email: richard.taylor@hotaka.t.u-tokyo.ac.jp)

G. Li, P. Ivanov, D.T.D. Childs, J. Sarma, N. Babazadeh, G. Terrnent, and R. A. Hogg are with the Department of Electronic and Electrical Engineering, the University of Glasgow, Rankine Building, Glasgow, G12 8LT, United Kingdom

T. S. Roberts, and B. Harrison are with Department of Electronic and Electrical Engineering, the University of Sheffield, Broad Lane, Sheffield, S3 7HQ, United Kingdom

Gelleta et.al, [16] recently investigated simulated effects of external feedback on PCSELs. With varying feedback intensity and phase to one side of a PCSEL (constant over the device side, but with varying values of phase shift), their model showed an influence on frequencies, threshold gain, gain margin, and field intensity. In this paper, we explore experimentally and theoretically the effect of external (in-plane) feedback on the lasing characteristics of all-semiconductor PCSELs. We begin by describing band-structure modelling which highlights the reduced mode frequency separation for triangular shaped PC features as compared to circular features. We then go on to describe a simple 1D model which predicts the effect of 1D feedback on the mode intensity within the PCSEL. We then go on to utilize a cleaved facet to introduce a distributed, varying facet phase across two orthogonal sides of the device (~4-5π distributed over ~450 periods (150 μm)). We describe the CW room temperature lasing characteristics of an all-semiconductor PCSEL and go on to discuss the effect of a single and second orthogonal cleave on the output characteristics of the device, and compare our results to theory.

II. DEVICE SIMULATION

In this section a photonic crystal is modelled by computing the definite frequency eigenstates of Maxwell's equations using fully vectoral plane wave expansion methods. The simulation is made using MIT photonic bands (MPB) [17], we consider the PC region to be infinite and to consist of InGaP and GaAs.

Figure 2 shows the TE photonic band diagram near the Γ point, and the inset shows an SEM micrograph of the PC (device realization is discussed in detail in the following section). The band structure is made up of two degenerate modes at lower frequencies and two non-degenerate (though closely spaced) modes to higher frequencies. Insets show the in-plane magnetic field distributions of each band at the gamma point for the positive and negative amplitudes of the magnetic fields in the direction perpendicular to the plane.

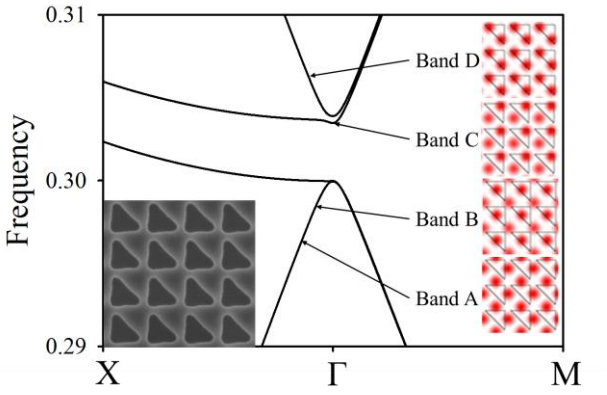

Figure 2 Simulated band structure of triangular PCSEL on a square lattice inset shows SEM of etched PCSEL region.

Figure 3 shows the dependence of Γ point band frequencies on the PC fill factor for (a) circular and (b) triangular atoms.

For both cases, as fill factor is increased, an increase in refractive index results in a monotonic reduction in mode frequencies.

As fill factor in circular PCs increases, we note a crossing of bands. This band crossing can result in a change from quadratic to linear dispersion at the Brillouin zone center and, if optimized, can lead to the realization of a laser with an accidental Dirac point. This is coincident with the degenerate/non-degenerate bands switching from the upper to the lower manifold. Accidental Dirac devices may exhibit many interesting phenomena [18-21].

For the PC with triangular features, we do not observe an intersection of bands. For the range where f<0.5 (corresponding to triangular holes in-filled with another material of higher refractive index) the high-frequency bands of are non-degenerate but closely spaced. Liang *at. al.*, [ref] demonstrated that moving to triangular PCs can give a difference in radiation constant (a mode loss) between modes which can give rise to enhanced single mode operation. However, the difference in radiation constant is small for many values of fill factor. As the gain spectrum of the active element can be expected to span these two bands, net modal gain is expected to be similar, for each mode, in cases where modes have similar radiation constants and are closely spaced. In these cases, competition between closely spaced modes is observed. However, it is worth noting that Gelleta et.,al. [16] demonstrated that lateral in-plane feedback can alter the threshold gain margin between photonic modes within the band structure.

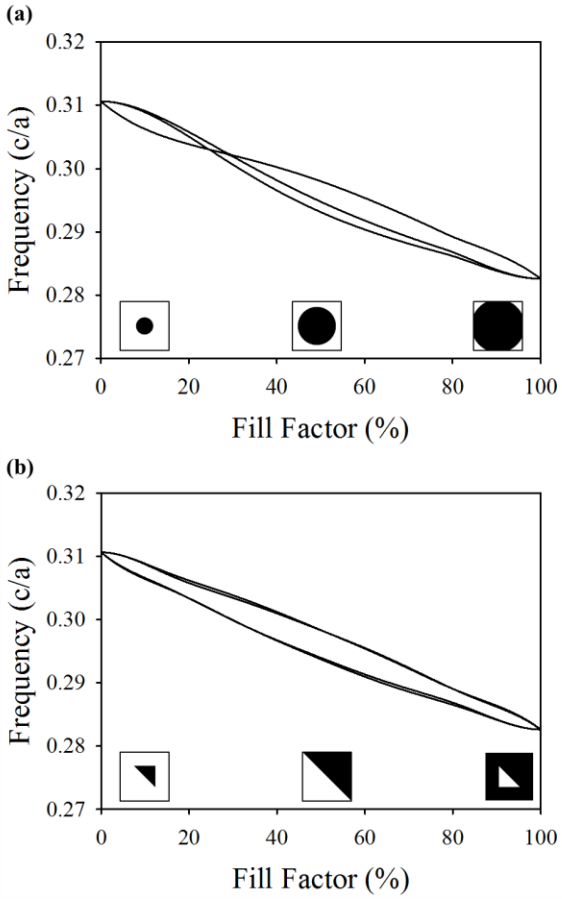

Figure 3 photonic crystal band frequencies as a function of fill factor for a) circular and b) triangular photonic crystals, where bands a, b, c, and d are the lowest to highest bands, respectively. Insets show a schematic representation of photonic crystal fill factors of 10,50, and 90%.

In order to investigate the spatial distribution of optical power within the PCSEL we adopt a simple model which considers the PCSEL structure as a 1D waveguide. For a given column of unit cells within the 2D PC, orthogonal in-plane scattering into and out of the column is considered to be equal. Orthogonal out-of-plane scatting is considered equivalent to an additional internal loss. A 1D model therefore provides a simple route to explore the effects of one dimensional feedback at the end of a column of PC unit cells.

The analysis is based on the transfer matrix method (TMM). Figure 4 shows a schematic representation of the layer structure simulated. The structure consists of a 1D periodically varying refractive index terminated by an air boundary, satisfying the piecewise homogeneous condition. Each period is characterized by a transfer matrix which represents the forward and backward travelling wave. An effective index method is used to calculate the vertical structural properties, where the effective index of each layer is calculated. A phase shift in external feedback is induced by varying the distance between the edge of the photonic crystal layer and the transparent semiconductor waveguide/air boundary, this distance is indicated by ϕ in fig. 4. Threshold is obtained by analysis of the matrix elements when both real and imaginary part of M_{11} become zero.

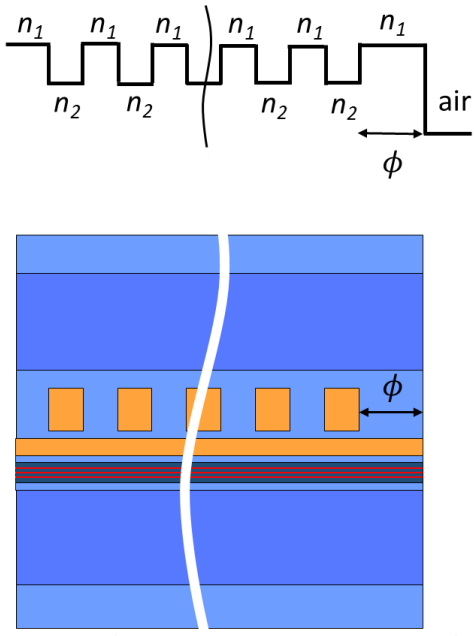

Figure 4 Schematic of simulated 1D PCSEL structure with refractive index

Figure 5 shows how the threshold gain changes as a function of reflection feedback phase for the fundamental (red) and second order mode (black). The phase shift is achieved in our model by varying the distance from photonic crystal region to the cleaved facet (Φ). Where the distance Φ varies from 392 nm to 549 nm giving a facet phase shift variation from –π to π. The blue and black dashed line represents the threshold gain of an uncleaved device for the fundamental (25.35 cm^{-1}), and second order mode (29.85cm^{-1}), respectively. The threshold gain margin for the uncleaved device is therefore 4.5cm^{-1}.

For the fundamental mode threshold gain varies cyclically as the phase shift is varied from -π to +π, the threshold gain reaches a minimum at $\frac{\pi}{2}$ and a maximum at $\frac{-\pi}{2}$. The threshold gain margin between the fundamental and second order mode is maximal for a facet phase of $\frac{\pi}{2}$. As may be expected, facet phase plays a key role in determining whether in plane feedback will increase or decrease lasing threshold. It also suggests that threshold gain margin can be increased with suitable facet phase.

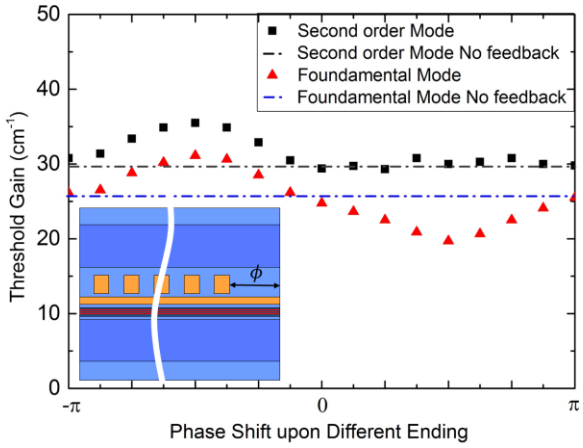

Figure 5 Simulated threshold gain of a 1D periodic structure for varying reflection phase for the fundamental (red) and second order mode (black). The inset shows a schematic representation of the structure considered with the distance from photonic crystal region to the cleaved facet (Φ) shown.

Figure 6 shows the 1D simulation of E^2 field distribution for a 150 μm wide PCSEL. In figure 6a the boundary of the photonic crystal is transparent waveguide. The envelope of the E^2 field distribution has a single peak in the center of the photonic crystal region and a symmetric broad distribution. Figure 6b shows the E^2 field distribution when the waveguide is terminated with air, simulating a cleaved facet at the edge of the photonic crystal. The distance between the PC edge and the air boundary is 494.2 nm giving a phase shift of $\frac{\pi}{2}$. The envelope of the E^2 field is observed to have a single peak which is shifted towards the cleave edge. The simulated structure in 6a with an air boundary layer shows significant narrowing of the envelope of the E^2 field distribution. This narrowing (by a factor of 2/3) suggests the far-field will be broadened by a factor of 3/2.

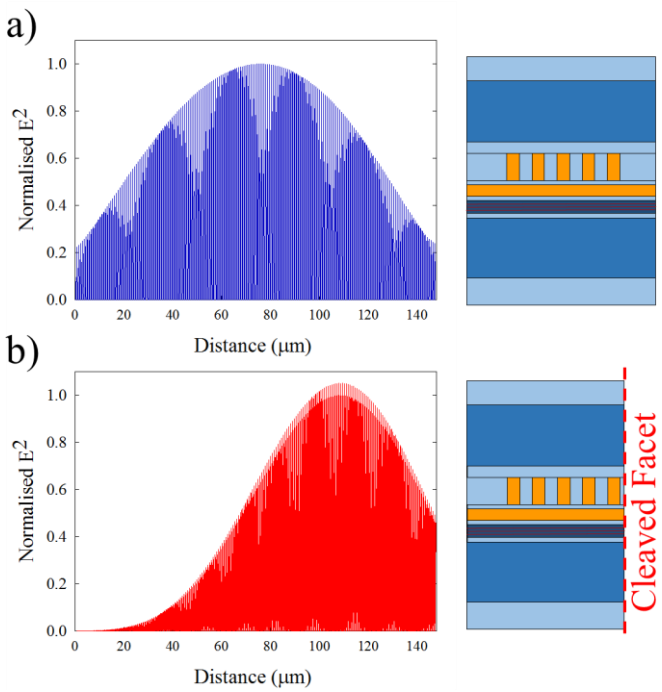

Figure 6 simulated E^2 field distribution of a 1D photonic crystal structure where the region around the photonic crystal is a) GaAs and b) air.

To summarize the simulation of feedback in 1D; The facet phase which produces the lowest threshold gain for the fundamental mode simultaneously produces the largest gain margin with the next lasing mode. Spatially, the introduction of feedback moves the center of the mode towards the origin of the feedback, and narrows the near-field envelope. These observations suggest that lateral feedback may not only be of importance in mode control, but contacted regions between PC and feedback element can provide electronic control of feedback, leading to future possible routes to all electronic beam shaping and divergence control.

III. DEVICE REALIZATION

Devices were grown by MOVPE on GaAs substrates cut 3° of (110). Initial growth consists of 1.5 μm n-type $Al_{0.4}Ga_{0.6}As$ lower cladding layer, 3 quantum well active region (8 nm $In_{0.2}Ga_{0.8}As$ QW's separated by 20 nm GaAs layers), a 40 nm p-$In_{0.48}Ga_{0.52}$ etch stop layer and a 150 $In_{0.48}Ga_{0.52}P$ layer (layer forms the PC region). The InGaP layer is patterned using electron beam lithography, where by right angled triangular holes are patterned into a SiO_2 hard mask. The pattern is transferred into the InGaP with a $Ch_4/H_2/O_2$ reactive ion etch. The complete PC area consists of 150 μm x 150 μm square area, where the PC consists of right angle triangles where the lattice constant of the PC is 288±1.1 nm and the ratio between the triangles' side and the lattice constant is 0.77 yielding a filling factor of 30%. Right angled triangles were chosen due to their apparent optimization of output power [6]. After etching, the wafer is cleaned using HF and placed back in the reactor. An overgrowth consisting of GaAs (to infill the holes and form the PC), a 1.5 μm p-type $Al_{0.4}Ga_{0.6}As$ upper cladding layer and finally a 400 nm p^+ GaAs cap layer. The growth parameters for this structure have been optimized elsewhere [11]. After over growth, devices were fabricated by etching a 100 μm diameter mesa through the p+ cap layer above the PC region, finally contacts were defined to provide a circular aperture with a diameter of 52 μm, as illustrated in fig. 1a. Figure 1a shows a 3D rendered cut away schematic representation of the PCSEL structure. Figure 1b shows a 1D schematic of the layer structure.

The completed structure consists of (from bottom to top) 1.5 μm n-type $Al_{0.4}Ga_{0.6}As$ lower cladding layer, 3 quantum well active region (8 nm $In_{0.2}Ga_{0.8}As$ QW's separated by 20 nm GaAs layers), a 40 nm p-$In_{0.48}Ga_{0.52}$ etch stop layer, 150 nm photonic crystal layer, p-type 1.5μm $Al_{0.4}Ga_{0.6}As$ cladding layer, finally a 400 nm p^+-type GaAs cap.

Cleaved facets are placed orthogonally along the edge of the photonic crystal region, providing lateral in-plane feedback with spatially varying feedback phase. Cleaved facet is placed along the edge of the PC region, giving a distance between the device mesa and the cleave of ~25 μm. Figure 8 shows a schematic of the photonic crystal lattice geometry indicating misalignment between PCSEL plane and cleave plane, in this device the misalignment provides a feedback phase variation of ~4-5π over the ~450 photonic crystal periods (150μm). Utilizing a distributed, varying feedback phase is expected to select the lowest threshold 2D mode due to the 2D nature of the PC feedback.

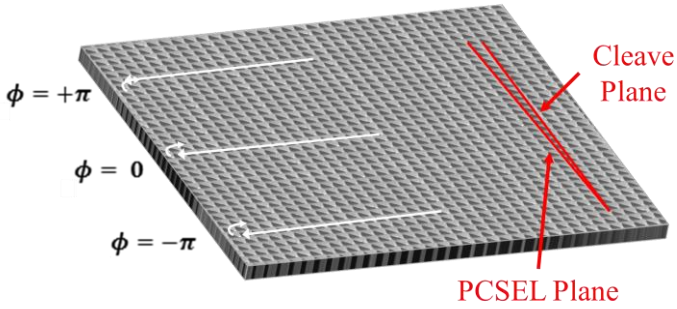

Figure 8 schematic showing photonic crystal lattice geometry indicating misalignment between PCSEL plane and cleave plane, showing in plane facet reflection phase.

IV. EXPERIMENTAL RESULTS

Figure 9b shows the CW room temperature LI of a PCSEL device, the device threshold is 112 mA (J=1.43 kA·cm^{-2}). The inset shows the far-field pattern which is symmetric with 1.2° divergence. Figure 9a plots the lasing spectra of the virgin device for current ranging from 100 to 200 mA. Two lasing modes at 963 nm and 963.5 nm are observed, with a total linewidth of ~1.5 nm. The two distinct modes are attributed to modes C and D in Figure 2.

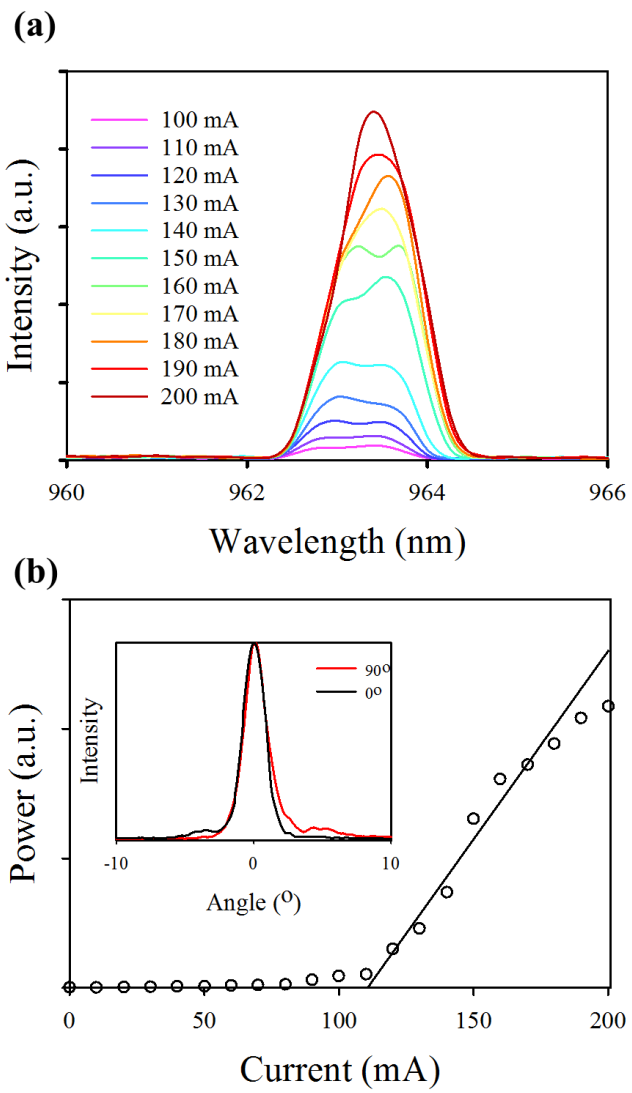

Figure 9 a) continuous wave EL spectra, b) LI of PCSEL device

Figure 10 shows the CW room-temperature LI of the virgin (black) PCSEL device, and with 1 (red), and 2 (blue) cleaves. With no cleave, the device has a threshold current of 112 mA (J=1.43 kA·cm^{-2}), the threshold is reduced to 88 mA (J=1.12 kA·cm^{-2}) when a single cleave in introduced to the PCSEL. The introduction of a second cleave does not reduce the threshold further, indicating that the lowest threshold 2D mode is selected by introducing external feedback to one side of the device. With additional feedback (one and 2 cleaves) an increased slope efficiency is also observed. In the cases where a cleaved facet is included, a non-linearity is observed as current is increased, the cause of such non-linearity requires further investigation but may be a result of the varying facet phase resulting in spatial threshold variation. Images show a 3D schematic representation of a PCSEL with no cleave, 1 cleave, and 2 cleaves.

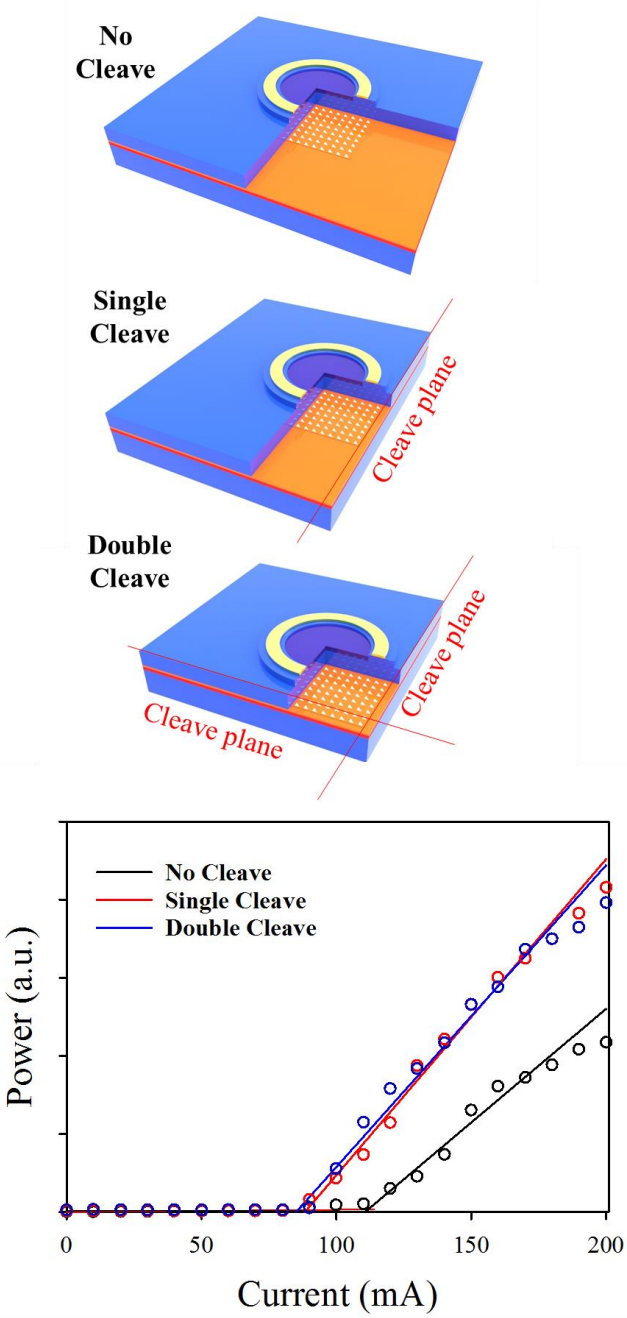

Figure 10 LI of the virgin (black) PCSEL device, and with 1 (red) and 2 (blue) cleaves.

Figure 11 shows the far-field at 1.1Ith for a PCSEL with no cleave (a), one cleave (b), and two cleaves (c). As described previously, for the virgin device, the far field pattern is shown to be symmetric, with a divergence of ~1.2°. With the addition of a single cleaved facet, the far field pattern of the device becomes asymmetric with divergence ~4° for the 90° (perpendicular to cleave) direction and ~1° for the 0° (parallel to cleave) direction. The addition of feedback clearly modifies the field distribution within the device. The addition of a second cleave results in a divergence of 0.8-1° indicating lasing is now taking place over a larger area of the PCSEL as compared to the virgin device.

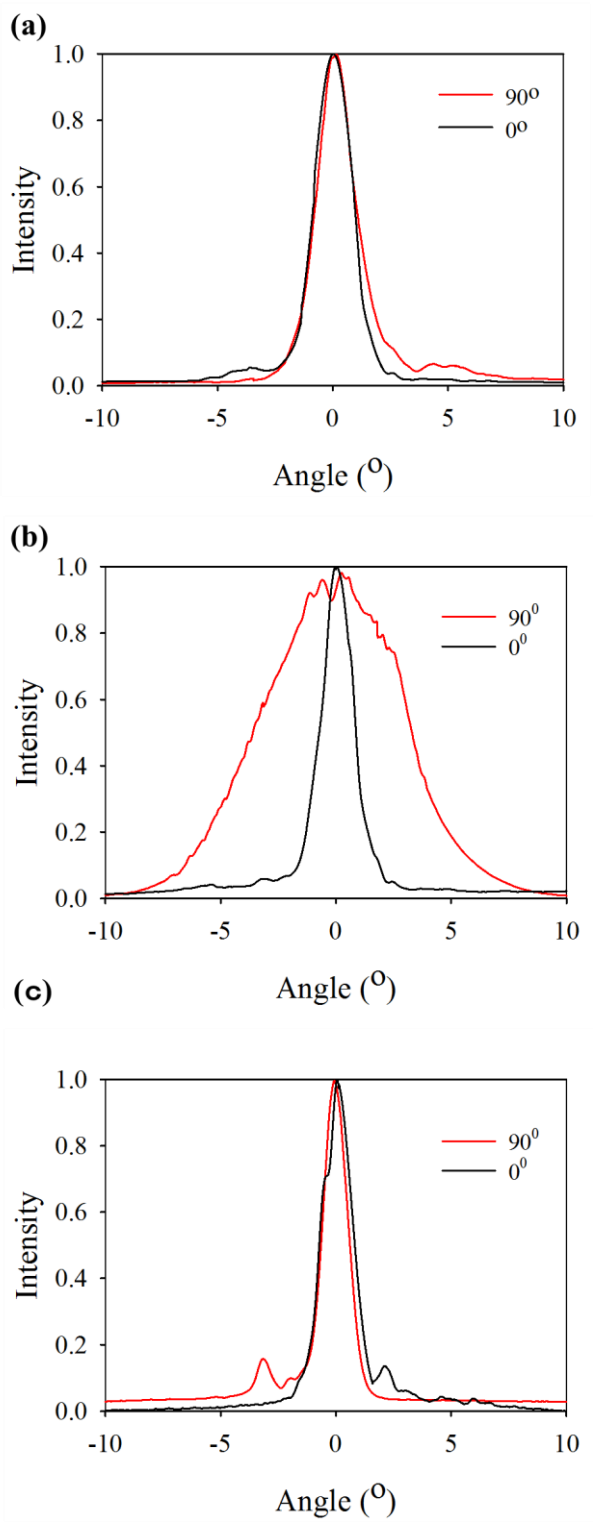

Figure 11 Far field pattern of PCSEL device (a) as fabricated, (b) with one cleave and, (c) with 2 cleaves

Figure 12 shows the CW room temperature EL spectra of the PCSEL device with no cleave (blue), 1 cleave (red), and 2 cleaves (black). As shown previously, the virgin device shows dual peak nature with peaks at 963 nm and 963.5 nm, with one cleave the spectra contains a single lasing peak at 963.75 nm. When a second cleave is introduced the peak wavelength increases to 964.2nm we attribute this to self-heating of the device caused by the 2 cleaves limiting the available area for heat dissipation to occur. However, we note that a shift in wavelength is an expected effect of lateral feedback [16]. We note that the spectral linewidth of the device remains broad after the inclusion of cleaved facets, and that this is similar to other all-semiconductor PCSELs [ref].

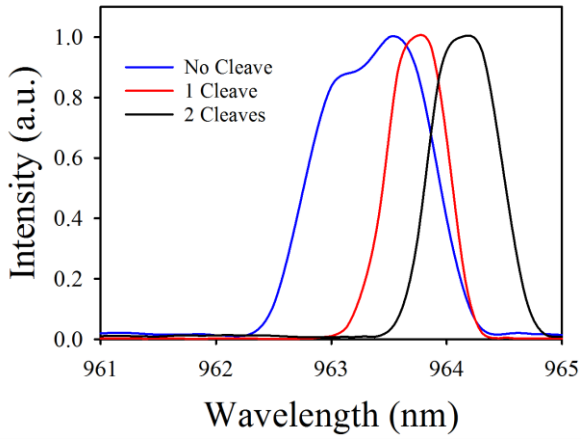

Figure 12 CW room temperature EL spectra for PCSEL device with no clave (blue), 1 cleave (red), and 2 cleaves (black).

Figure 13 shows the peak wavelength as a function of current for a PCSEL device with no cleave, 1 cleave, and 2 cleaves. In each case the peak wavelength slightly increases as the applied current increases. For the virgin device two lasing modes of ~963 nm and ~963.5 nm are observed. The two distinct modes are attributed to modes C and D in Figure 2. The introduction of a single cleave results in single-mode behavior with a red-shift of the lasing peak of ~0.25 nm. Single mode operation with a red-shift of ~0.65 nm is observed for the case of two cleaves. For both one and two cleaves, single mode operation is maintained over all measured drive currents (up to 200 mA (2.55 kA·cm^{-2})). As we have drastically changed the heatsinking of the devices we cannot rule out self-heating to be the cause of this redshift (~7 and 17° increase in junction temperature for the single and double cleaved device, respectively [10]).

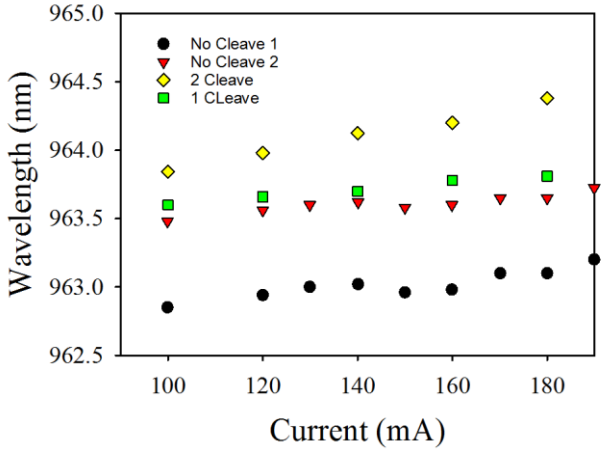

Figure 13 peak wavelength as a function of current for a PCSEL structure with no cleave (black/red), 1 cleave (green), 2 cleaves (red).

It is clear that mode selection is possible through the use of lateral feedback. As we have a distributed feedback phase, competition would be expected not necessarily to the next mode, but to slightly different feedback phases of the same mode. In the case of strong feedback (R=1), there is a significant change in lasing wavelength with varying feedback phase [16], in this case we have and estimated reflectivity at the cleave plane of 0.559. Spectral broadening of the lasing wavelength with increasing drive current may therefore be expected. However, recent work on spatial coherence effects in PCSELs suggest that injection locking occurs for large area PCSELs with a spatial variation of PC shape/period [22] and for individual PCSELs making up coupled arrays [5,22,23]. Further theoretical and experimental work is required to explore the mode stability under high power operation.

In order to harness feedback effects in a scalable manner, the PCSEL would need to be terminated with a DBR boundary. The incorporation of an electrically contacted coupling waveguide region [5, 24, 25] allows us to envisage electronic control of the feedback amplitude and phase, allowing all-electronic control of lasing position and beam divergence [24, 25].

V. Conclusions

In summary, an all semiconductor PCSEL based on epitaxial overgrowth with a square lattice of triangles has been studied theoretically and experimentally under a range of feedback regimes. Feedback to a single side of the device results in the selection of the lowest threshold 2D lasing mode and a modification to the field distribution within the device resulting in a broadening to the far-field in one direction. For an originally dual-mode laser, single mode operation is obtained over a larger area through the introduction of feedback to two facets.

References

[1] M. Imada, S. Noda, A. Chutinan, T. Tokuda, M. Murata and a. G. Sasaki, "Coherent two-dimensional lasing action in surface-emitting laser with triangular-lattice photonic crystal structure," Applied Physics Letters, vol. 75, pp. 316-318, 1999.

[2] D. Ohnishi, T. Okano, M. Imada and S. Noda, "Room temperature continuous wave operation of a surface emitting two dimensional photonic crystal laser," optics express, vol. 12, no. 8, p. 1562, 2004.

[3] S. Noda, M. Yokoyama, A. Chutinan, M. Imada and M. Mochizuki, "Polarization Mode Control of Two-Dimensional Photonic Crystal Laser by Unit Cell Structure Design," Science, vol. 293, p. 1123, 2001.

[4] E. Miyai, K. Sakai, T. Okano, W. Kunishi, D. Ohnishi and a. S. Noda, "Lasers producing tailored beams," Nature, vol. 441, p. 946, 2006.

[5] R. Taylor, D. Child, P. Ivanov, B. Stevens, N. Babazadeh, A. Crombie, S. T. G. Ternent, H. Zhou and R. Hogg, "Electronic control of coherence in a two-dimensional array of photonic crystal surface emitting lasers," Scientific Reports, vol. 5, p. 13203, 2015.

[6] K. Hirose, Y. Liang, Y. Kurosaka, A. Watanabe, T. Sugiyama and S. Noda, "Watt-class high-power, high-beam-quality photonic-crystal lasers," Nature Photonics, vol. 8, pp. 406-411, 2014.

[7] Y. Liang, C. Peng, K. Sakai, S. Iwahashi, S. Noda, "Three-dimensional coupled-wave model for square-lattice photonic crystal lasers with transverse electric polarization: A general approach," Physical Review B 84, 195119, 2011

[8] S. Noda, M. Yokoyama, A. Chutinan, M. Imada and a. M. Mochizuki, "Polarization mode control of two-dimensional photonic crystal laser by unit cell structure design," Science, vol. 293, pp. 1123-1125, 2001.

[9] Y. Kurosaka, S. Iwahashi, Y. Liang, K. Sakai, E.Miyai, W. Kunishi, D. Ohnishi and S. Noda, "On-chip beam-steering photonic-crystal lasers," Nature Photonics, vol. 4, pp. 447-450, 2010.

[10] D. Williams, K. Groom, D. Childs, R. Taylor, S. Khamas, R. Hogg, B. Stevens, N. Ikeda and Y. Sugimoto, "Epitaxially regrown GaAs-based photonic crystal surface emitting laser," Photonics Technology Letters, vol. 24, no. 11, pp. 966-968, 2012.

[11] D. Williams, K. Groom, D. Childs, R. Taylor, S. Khamas, R. Hogg, B. Stevens, N. Ikeda and Y. Sugimoto, "Optimisation of coupling between photonic crystal and active elements in an epitaxially regrown GaAs based photonic crystal surface emitting laser," Japanese Journal of Applied Physics, vol. 52, no. 02BG05-1-3, 2012.

[12] R. J. E. Taylor, D. M. Williams, J. R. Orchard, D. T. Childs, S. Khamas and R. Hogg, "Band structure and waveguide modelling of epitaxially regrown photonic crystal surface emitting lasers," Journal of Physics D, vol. 46, no. 26, p. 264005, 2013.

[13] R. Taylor, D. Williams, D. Childs, B. Stevens, L. Shepherd, S. Khamas, K. Groom and R. Hogg, "All-semiconductor photonic crystal surface emitting lasers based on epitaxial regrowth," IEEE Journal of Selected Topics in Quantum Electronics, vol. 19, no. 4, p. 4900407, 2013.

[14] M. Nishimoto, K. Ishizaki, K. Maekawa, K. Kitamur and S. Noda, "Air-Hole Retained Growth by Molecular Beam Epitaxy for Fabricating GaAs-Based Photonic-Crystal Lasers," Applied physics express, vol. 6, no. 4, 2013.

[15] M. Nishimoto, K. Ishizaki, K. Maekawa, Y. Liang, K. Kitamur and a. S. Noda, "Fabrication of Photonic Crystal Lasers by MBE Air-Hole Retained Growth," Applied physics express, vol. 6 , no. 4, 2013.

[16] J. Gelleta, Y. Liang, H. Kitagawa and a. S. Noda, "Influence of external reflection on the TE mode of photonic crystal surface-emitting lasers," Journal of the Optical Society of America B, vol. 32, pp. 1435-1441, 2015.

[17] S. G. Johnson and J. D. and Joannopoulos, "Block-Iterative Frequency-Domain Methods for Maxwell's Equations in a Planewave Basis," Optics Express, vol. 8, no. 3, pp. 173-190, 2001.

[18] X. Huang, Y. Lai, Z. Hong Hang, H. Zheng, and C. T. Chan, "Dirac Cones Induced by Accidental Degeneracy in Photonic Crystals and Zero-Refractive-Index Materials", Nature Materials, 10, 582–586, 2011.

[19] R. A. Sepkhanov, Ya. B. Bazaliy, and C. W. J. Beenakker, "Extremal Transmission at the Dirac Point of a Photonic Band Structure", Phys. Rev. A 75, 063813, 2007.

[20] X. Zhang, "Observing Zitterbewegung for Photons near the Dirac Point of a Two-Dimensional Photonic Crystal", Phys. Rev. Lett. 100, 113903, 2008

[21] S. Chua, L. Lu, J. Bravo-Abad, J. D. Joannopoulos, and M. Soljačić, "Larger-area single-mode photonic crystal surface-emitting lasers enabled by an accidental Dirac point", Optics Letters Vol. 39, Issue 7, pp. 2072-2075, 2014.

[22] M. De Zoysa, T. Kobayashi, M. Yoshida, M. Kawasaki, K. Ishizaki, R. Hatsuda and S. and Noda, "In-plane mutual wavelength locking of photonic crystal lasers," in International Semiconductors Lasers Conference, Kobe, 2016.

[23] R. Taylor, D. Childs and R. and Hogg, "Improved Laser Design". Patent 14149843, 2014.

[24] R. T. D. R. Hogg, "laser device and methods for its operation". Patent MJN/BP7194269, 2016.

[25] R. Taylor, D. Childs, P. Ivanov, B. Stevens, N. Babazadeh, J. Sarma, S. Khamas, A. Crombie, G. Li, G.Ternent, S. Thoms, H. Zhou and R. Hogg, "Coherently Coupled Photonic Crystal Surface Emitting Laser Array," Journal of selected topics in quantum electronics, vol. 21, no. 6, pp. 4900307, 2015

Richard J.E. Taylor received the B.Eng. degree in electrical engineering in 2010, the M.Sc. degree in semiconductor photonics in 2011 and the Ph.D. degree in photonic crystal surface emitting lasers in 2015, from the Electronic and Electrical Department, The University of Sheffield, Sheffield, U.K. Upon completion of his Ph.D. Richard was awarded the EPSRC doctoral prize fellowship at the University of Sheffield.

He is currently a JSPS Postdoctoral Research Fellow at the University of Tokyo, Tokyo, Japan.

Guangrui Li received the B.Eng. degree in electrical engineering and automation in 2013 from Fudan University, Shanghai, China. Going on to gain the M.Sc. degree in 2014 in semiconductor photonics from the University of Sheffield, Sheffield, U.K. He is now working towards the Ph.D. degree in photonic crystal surface emitting lasers in the University of Glasgow.

Pavlo Ivanov received the Dipl.-Ing. degree in electrical engineering (with honours) from Kharkiv National University of Radio and Electronics, Kharkiv, Ukraine, in 1999, and the Ph.D. degree in Optics and Laser Physics from Kharkiv National University, Kharkiv, Ukraine, in 2004.

In 2003-2011, he was as a Visiting Fellow, Research Assistant, Research Associate and a GWR Research Fellow of the University of Bristol, Bristol, U.K. During this time he has been involved in theoretical and experimental investigation of photonic crystal displays and VCSELs incorporating two-dimensional photonic crystals. In 2012-2013, he was a Research Associate of the University of Leeds, Leeds, UK, working on modelling of SiGe quantum cascade lasers. In 2013-2015, as a Research Associate he was with the University of Sheffield, Sheffield, UK, and in 2015 he joined the University of Glasgow, Glasgow, UK.

His current interests include of theory and modelling of semiconductor light-emitting devices, high-performance computing, postprocessing of devices using focused ion beam systems, experimental study of laser device characteristics and optical systems.

David T.D. Childs (M'15) received the B.Sc. degree in Physics, the. M.Sc. degree in Semiconductor Science and Technology from Imperial College, London in 1996 and 1997 respectively. He continued at Imperial where he received his PhD in Properties and applications of 1.3um InAs/GaAs Quantum Dot Devices in 2002.

He was then with the R&D Department of Marconi Optical Components (latter Bookham, now Oclaro) at the Caswell semiconductor research and fabrication facility until 2006, where he was responsible for the development of a range of telecoms lasers. During this time he also worked on several European projects developing Quantum Dot technology. Following this he joined the department of Electronic and Electrical Engineering at the University of Sheffield. There he was engaged in a number of projects developing semiconductor light sources from visible through to THz wavelengths. He was also involved in developing systems to demonstrate the application of semiconductor devices to fields ranging from selective laser melting (3D printing), to mid-infrared hyper-spectral imaging (biomedical imaging). Since 2015 he is a lecturer in the Electronic and Nanoscale Engineering group within the School of Engineering at the University of Glasgow. He has contributed to over 100 journal and conference publications. His research interests span from semiconductor light emitter development through photonic integration to the applications of these devices and systems from communications to biomedicine.

Tim S. Roberts received the M.Eng. degree in microelectronics from the University of Sheffield, Sheffield, U.K., in 2013, where he is currently working toward the Ph.D. degree in MOVPE growth of Quantum Dots.

Ben J. Stevens was awarded his PhD in 2010 from the University of Sheffield on advanced GaAs based lasers. During his PhD he was awarded a Japanese Society for the Promotion of Science summer fellowship, which he spent in the Asakawa group in Tsukuba learning selective area MBE. From 2009 to 2016 he was employed at the National Centre for III-V Technologies where he was responsible for the development of MOVPE growth.

Bret Harrison Received a Master of Engineering degree in Microelectronics in 2013 from the University of Sheffield. He is currently working for the National Centre for III-V Technologies as a metal organic vapour phase epitaxy research engineer. His main research interests are the realisation of advanced group III Arsenide/Phosphide based optical-electronic devices including resonant tunnelling diodes, photonic crystal surface emitting lasers and semiconducting disk lasers.

Jay Sarma obtained the B.Eng. degree in electronics & telecomn eng. from Jadavpur Universty, Calcutta, India , MS in electrical eng. from the Illinois Inst. of Technology, Chicago, USA, and the Ph.D from the dept.of electronics & electrical eng., Univ.Leeds, UK. He was then a National Research Council of Canada postdoctoral research fellow at the Communications Research Centre in Ottawa before he returned to the U.K. and worked as Research Associate at the universities of Sheffield, Liverpool, and Bath. He was appointed as a member of academic staff at the Univ.of Bath where he led a research group working on guided-wave photonics until he retired as Reader from the university.

Nasser Babazadeh obtained his PhD in 2010 from the University of Sheffield and then began working as postdoctoral researcher with the Department of Electronic and Electrical Engineering, the University of Sheffield. Since 2015 he has worked as a post-doctoral research associate within the School of Engineering at the University of Glasgow. His research is in the area of semiconductor nanostructures, with emphasis on quantum dot, quantum well structures including, VCSELS/VECSELS and Super luminescent diodes (SLDs).

Gary Terrnent received the BEng degree in Electrical and Electronic Engineering in 1993 and then a PhD developing Si/SiGe RF Technology in 2000 from the University of Glasgow. He was a project engineer at IBM in Greenock, U.K. and a semiconductor device engineer at Siemens Microelectronics in North Tyneside. He was the lead development engineer for 6 years at Intense Ltd, where he patented a number of laser printing devices. He was product

manager at Xanic Ltd developing MMICs for the defense markets. He managed the activities of the EPSRC nanofabrication centre for III-V technologies at Glasgow. His research interests are device engineering and fabrication of electronic and optical semiconductor devices He is currently a research fellow at the University of Glasgow developing DFB lasers for Quantum Technology.

Richard A. Hogg Obtained his PhD in Physics in 1995 from the University of Sheffield and then spent two years as a postdoctoral researcher at NTT Basic Research Laboratories in Atsugi, Japan. He was then awarded an EU-Japan fellowship as a visiting researcher in Professor Arakawa's Laboratory at the University of Tokyo. He subsequently spent three years at Toshiba Research Europe's Cambridge Laboratory, before moving to Agilent Technologies Fibre-Optic Component Operation in Ipswich, UK, in 2000. In 2003 he joined the Electronic and Electrical Engineering Department of the University of Sheffield. In 2015 he became Professor of Electronic and Nanoscale Engineering at the University of Glasgow. His research group is active in developing the understanding of device physics and engineering, epitaxial processes fabrication technologies, and applications of various semiconductor laser, amplifier, and super-luminescent diode devices.